Energy 134 (2017) 649–658

Contents lists available at ScienceDirect

Energy

journal homepage: www.elsevier.com/locate/energy

The economics of electricity generation from Gulf Stream currents

Binghui Li [a, *], Anderson Rodrigo de Queiroz [a], Joseph F. DeCarolis [a], John Bane [b], Ruoying He [c], Andrew G. Keeler [d], Vincent S. Neary [e]

[a] Department of Civil, Construction, & Environmental Engineering, North Carolina State University, Raleigh, NC, 27695-7908, United States
[b] Department of Marine Sciences, University of North Carolina, Chapel Hill, NC, 27599-3300, United States
[c] Department of Marine, Earth, and Atmospheric Sciences, North Carolina State University, Raleigh, NC, 27695-7908, United States
[d] UNC Coastal Studies Institute, Wanchese, NC, 27981, United States
[e] Water Power Technologies Department, Sandia National Laboratory, Albuquerque, NM, 87123, United States

ARTICLE INFO

Article history:
Received 6 January 2017
Received in revised form
27 May 2017
Accepted 9 June 2017
Available online 9 June 2017

Keywords:
Ocean current energy
Gulf Stream
Portfolio optimization
Energy economics
Renewable generation

ABSTRACT

Hydrokinetic turbines harnessing energy from ocean currents represent a potential low carbon electricity source. This study provides a detailed techno-economic assessment of ocean turbines operating in the Gulf Stream off the North Carolina coast. Using hindcast data from a high-resolution ocean circulation model in conjunction with the US Department of Energy's reference model 4 (RM4) for ocean turbines, we examine resource quality and apply portfolio optimization to identify the best candidate sites for ocean turbine deployment. We find that the lowest average levelized cost of electricity (LCOE) from a single site can reach 400 $/MWh. By optimally selecting geographically dispersed sites and taking advantage of economies of scale, the variations in total energy output can be reduced by an order of magnitude while keeping the LCOE below 300 $/MWh. Power take-off and transmission infrastructure are the largest cost drivers, and variation in resource quality can have a significant influence on the project LCOE. While this study focuses on a limited spatial domain, it provides a framework to assess the techno-economic feasibility of ocean current energy in other western boundary currents.

1. Introduction

Marine energy resources, which include ocean waves, tides, open ocean currents as well as gradients in ocean temperature [1] and salinity [2], could serve as an important low carbon renewable energy source. Previous research has shown great potential for marine electricity generation worldwide [3–9]. The available kinetic energy in US coastal waters associated with wave, tidal, and ocean current energy resources is estimated to be 1170 TWh/yr [8], 222–334 TWh/yr [9] and 45–163 TWhyr [7], respectively.

Ocean currents (i.e., non-tidal marine currents) are seawater circulations driven by a combination of wind, density, and pressure differences in the ocean [1]. Ocean currents mostly flow horizontally and typically have their highest flow velocities near the surface. On average, they will have a prevailing direction, but temporal variability can at times be strong. Ocean currents have been studied over the past several decades as a potential energy source for electricity generation, especially the Gulf Stream [5–7,10–12], the Kuroshio Current [13,14], and the Agulhas Current [15–17]. These are all jet-like oceanic western boundary currents, which are among the swiftest large-scale marine currents. Their current speeds are fast enough to be considered excellent energy resources [11,18]. These western boundary currents typically are thousands of km in length, about 100 km wide, extend to at least 1000 m depth, and have the strongest current speed at the surface near the center of the current [11].

As the most intensely studied ocean current, the Gulf Stream begins in the Caribbean and terminates in the North Atlantic Ocean. This fast moving ocean current brings a significant amount of heat and salt to the European continent, and also provides an opportunity for energy capture. In the US, the most plausible locations to harness Gulf Stream energy are in the Florida Straits and off the North Carolina coast, the two locations where the current makes its closest approach to shore. The estimated extractable energy from the Florida Current (i.e., the portion of the Gulf Stream within the Florida Straits) ranges from 1 GW to 10 GW [5–7], and the portion of the Gulf Stream within 200 miles of the US coastline between Florida and North Carolina can yield approximately 9 GW or

* Corresponding author.
E-mail address: bli6@ncsu.edu (B. Li).

http://dx.doi.org/10.1016/j.energy.2017.06.048
0360-5442/

80 TWh per year of electrical power [7].

Most ocean currents exhibit some degree of path meandering [19–25] as well as periods of acceleration and deceleration. As a consequence, the ocean current velocity at a specific location is subject to temporal variability [26]. Previous studies [19,23,24,27] have shown that the lateral movements of the Gulf Stream from the Florida Straits to Cape Hatteras, NC can be significant due to wind forcing, flow instabilities, and bathymetric effects. Along the southeastern US coast, the standard deviation of the lateral Gulf Stream position displacement increases from 5 to 10 km within the Florida Straits to an approximate 40 km local maximum downstream of a bottom topographic feature off Charleston, SC known as the "Charleston Bump" (31°–32° N latitude). The standard deviation in the Stream's lateral displacement decreases moving northeastward (downstream) from the Bump, to approximately 10–20 km at Cape Hatteras, NC. These path variations will influence the cost-effectiveness of Gulf Stream energy extraction.

Previous work includes technical assessments of marine turbine design and performance, mostly to address tidal energy applications [28–35]. In addition, a detailed cost analysis for a hypothetical project in the Florida Straits has been performed [10,36]. However, the Florida Current is confined within the Florida Straits, which is approximately 100 km wide between the Florida peninsula and the Bahama Banks. By contrast, significant meanders are observed for the Gulf Stream off the North Carolina coast [11,19]. While resource assessments conducted at several discrete locations near Cape Hatteras, NC indicate potential for commercial development [11,37], they do not tie ocean current resource estimates to the economic performance of turbine arrays.

This paper represents a significant extension of existing work by providing a comprehensive techno-economic assessment of ocean current energy off the North Carolina coast. Our analysis is the first to combine a multi-year resource assessment based on output from a high-resolution ocean circulation model, a portfolio optimization to identify optimal locations to install turbine arrays, and a levelized cost analysis that considers the tradeoff between resource quality and distance to shore. Furthermore, this paper represents the first application of portfolio optimization in order to identify a diverse set of generation sites that hedge against the risk of future Gulf Stream meanders. The structure is as follows. Section 2 describes the model assumptions used for resource assessment and the techno-economic study, and introduces the portfolio optimization model. The results are presented in Section 3, and Section 4 describes the insights and conclusions from this study.

2. Methods

2.1. Resource characterization

Gulf Stream resource data is obtained from a realistic high-resolution regional ocean circulation model, which is used to hindcast the circulation of the Middle Atlantic Bight (MAB), South Atlantic Bight (SAB) and parts of Gulf Stream, Slope Sea, and Sargasso Sea [38]. The MABSAB model is based on the Regional Ocean Modeling System (ROMS), a free-surface, terrain-following, primitive equations ocean model in widespread use for estuarine, coastal, and regional ocean-wide applications [38]. The MABSAB model covers the domain from 81.89° W to 69.80° W, 28.41° N to 41.84° N. The horizontal resolution is approximately 2 km. Depth is represented by 36 terrain-following layers [38].

Model bathymetry was interpolated from National Geophysical Data Center (NGDC) 2-Minute Gridded Global Relief Data. Momentum advection equations were solved using a third order upstream bias scheme for three-dimensional velocity and a fourth-order centered scheme for two-dimensional transport, whereas tracer (temperature and salinity) advections were solved with a third-order upstream scheme in the horizontal direction and a fourth-order centered scheme in the vertical direction. The horizontal mixing for both the momentum and tracer utilized the harmonic formulation with 100 and 20 m^2/s as the momentum and tracer mixing coefficient, respectively. Turbulent mixing for both momentum and tracers was computed using the Mellor/Yamada Level-2.5 closure scheme [39]. For open boundary conditions, the model was nested inside the 1/12° global data assimilative HYCOM/NCODA [40] output superimposed with the 6 major tidal constituent forcing derived from an ADCIRC tidal model [41] simulation of the western Atlantic.

The MABSAB sub-domain selected for analysis was 77° W to 74° W, 33° N to 36° N, which includes the strongest, near-shore Gulf Stream current off the North Carolina coast. While the fastest Gulf Stream currents are closest to the surface, we assume the turbines are installed at a depth of approximately 50 m below the sea surface to accommodate the drafts of large ships and to keep turbine hardware out of the surface wave zone. The study domain is shown in Fig. 1: the 334 km × 280 km rectangle is discretized into a 2 km × 2 km mesh grid with 19,188 grid points. Daily average current speeds for the years 2009–2014 are used in this study [38,42,43].

The electricity output of the turbine at a given current velocity is expressed by the following equation:

$$P(v) = \frac{1}{2}\eta C_p \rho A v^3 \tag{1}$$

where v is the current velocity, A is the swept rotor area, ρ is the density of sea water, C_p is the power coefficient that accounts for the conversion of current power to mechanical power, and η is the combined power chain conversion efficiency, which includes the gearbox, generator, transformer and power inverter efficiencies (see Supplementary Table F for values of the parameters). The design and performance of the ocean current turbine is adopted from Neary et al. [10]. The design represents a moored glider with four axial flow marine turbines. The rated capacity of each turbine is 1 MW, and the total capacity of each unit is 4 MW. The power curve is adapted from Neary et al. [10] but adjusted for the lower

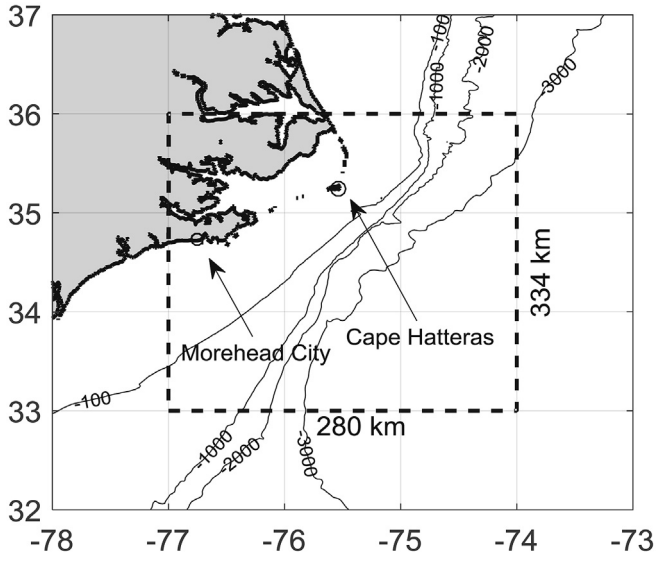

Fig. 1. The study domain near the North Carolina coast, as represented by a dashed box. The assumed grid tie-in point is located at Morehead City, NC, which is marked with a circle. Isobaths are shown in meters.

average current velocity encountered off the North Carolina coast (Supplementary Figure C). Similar to a wind turbine, the maximum electricity production of each turbine is limited by the installed generator capacity. We also assume that the space between neighboring units is 1 km, and for simplicity, the wake from upstream units does not affect the performance of downstream units [10]. Given this configuration, the average installed capacity in a single 2 km × 2 km grid cell is 16 MW. See Supplementary Fig. B for a detailed layout of generation units.

The site-specific annual electricity production (E_{ij}) at grid (i,j) is obtained by integrating the product of the turbine's output at a specific current velocity, $P(v)$, with the velocity probability density, $\Pr(v)_{ij}$, over the entire velocity interval:

$$E_{ij} = AF \cdot \eta_{TL} \cdot 8760 \int_0^{v_{max}} P(v) \cdot \Pr(v)_{ij} \mathrm{d}v \quad (2)$$

where, AF is the annual availability factor and η_{TL} is the transmission line efficiency. A discretized probability distribution was obtained by binning the daily average velocities from the MABSAB model over the entire 6-year period into a set of velocity ranges. The velocity probability distribution is provided in Supplementary Fig. C, along with the assumed power curve.

The estimated annual electricity production is used to calculate the corresponding site-specific capacity factors. The capacity factor (CF) at each site is defined as the ratio of its estimated annual electricity production to its maximum annual electricity production, if it operated continuously at its full capacity. A higher site-specific capacity factor implies higher electricity production given the same amount of installed capacity.

2.2. Portfolio optimization procedure

In order to optimize the locations for marine current turbine deployment, we apply mean-variance portfolio (MVP) theory to create a portfolio consisting of multiple geographically diversified sites. MVP theory was developed by Markowitz [44] as a way to devise an efficient financial portfolio consisting of different assets. An efficient portfolio is the one with the least portfolio risk (typically modeled as total variance [45,46], or coefficient of variation [47]) at a specified level of expected returns, such that one cannot decrease the portfolio risk while increasing the expected return level.

MVP has been used to optimally site energy technologies, most notably wind farms. Spreading wind farms over a wide geographic area can decrease fluctuations in aggregate output and improve overall economic viability [45,46]. For example, Roques et al. [46] used historical wind production data from several European countries and applied MVP to optimally allocate wind farm capacity in order to minimize the total variance associated with specific electricity generation targets.

MVP has also been applied to the repowering of existing wind farms in Spain [48]. Santos-Alamillos et al. [48] find that portfolio optimization can increase electricity production by 16–55% while reducing the hourly fluctuations in output by 12–31%. In Novacheck and Johnson [49], different optimal wind portfolios were tested in a unit-commitment and dispatch model representing the US Midwest power system in order to evaluate the value of reduced variability to the system. Wind power generation smoothing was also investigated with MVP considering turbine failures and correlation between aggregated wind power output and electricity demand [50]. Other works focus on using MVP to achieve an optimal investment plan involving multiple energy resources [51] and to identify the best combined heat and power generation technologies based on the net present value of different portfolios [52]. To our knowledge, our work is the first attempt to apply MVP to identify optimal allocation of hydrokinetic turbines.

In our study, the installed turbine capacity is optimally distributed across sites (i.e., grid cells) within the study domain to form a portfolio. We wish to achieve a pre-determined system target capacity factor – analogous to the expected return – while minimizing total variance in aggregate output, which serves as a measure of system risk. In addition, we add the following constraints: (1) the number of turbine units installed in a single grid cell must be an integer and cannot exceed a maximum of four units per cell or 16 MW, (2) the investor may limit the number of selected grid cells within an appropriate range, and (3) the investor may fix the total installed capacity of the project. In addition, the anchoring system limits the seabed depth [53], so we assume that the turbines can only be installed where the seabed depth is between 100 m and 2500 m.

With all the information above, we construct a 2-stage optimization model (see Supplementary Notes 1 for the model formulation). We assume that a marine current installation with a total capacity of 80 MW will be deployed across a maximum of 5 sites, with the installed capacity within each site less than or equal to 16 MW. This scenario represents a plausible utility scale deployment of generating units. The implementation of the 2-stage model is developed using MATLAB and CPLEX on a workstation with 24 cores and 256 GB of memory.

2.3. Economic assumptions

Costs associated with Gulf Stream project development draw heavily on the RM4 marine turbine design detailed in Neary et al. [10]. The design of the RM4 marine turbine involved rigorous analysis, including the specification of individual parts associated with subcomponents and validation through scaled model experiments. Emphasis was placed on simple designs using conventional materials, and to the extent possible, commercial off-the-shelf (COTS) components. Thus the cost and performance assumptions embedded in the RM4 design are deliberately conservative. Future innovations (e.g., advanced control strategies or advanced materials) could improve the assumed techno-economic performance.

The capital cost consists of pre-installation development, structural device components, power take-off, infrastructure, and project deployment costs, as shown in Supplementary Table G. Annual recurring costs include project operation and maintenance costs and recurring environment monitoring costs, as shown in Supplementary Table H. Given the lack of commercial experience with this technology, we emphasize that substantial cost uncertainty exists, particularly given the need to operate in a harsh marine environment.

All capital costs incurred at the beginning of the project are multiplied by the capital charge rate (CCR) to calculate the annual payments required to pay off that investment over the assumed project lifetime. The lifetime of the project is assumed to be 30 years, based on the typical assumed lifetimes for marine energy projects. A discount rate of 10% is used to represent the cost of capital to an investor or utility.

Due to limited commercially available data for marine hydrokinetic turbines, the capital costs for the structural device components and power take-off are based on Neary et al. [10]. We subsequently compared the assumed capital cost with Verdant Power's estimate for the Roosevelt Island Tidal Energy (RITE) project [54] and found that the percentage difference between the two estimates is only 0.2%.

The cost of infrastructure consists of two major parts: the cost of

the dedicated operations and maintenance (O&M) vessel and the cost of the transmission system. The cost for the required electricity transmission is drawn from a similar project with undersea cables tied to the North Carolina grid [55]. We assume the transmission system can be divided into two subsystems: a collection subsystem, which transmits electricity from the turbines to the collection point, rated at a medium voltage of 33 kV; and a transmission subsystem, which steps up the voltage to 132 kV and transmits the power received at the collection point to the onshore grid tie-in point [56]. The collection point is the hub that aggregates electricity from all the spur lines. To calculate transmission cable distances, the model assumes that the connection to the grid is located in Morehead City, NC, where existing transmission and distribution infrastructure exists [57]. Therefore, the total transmission cost is a function of the total collection cable length, total transmission cable distance, and number of installed units. See Supplementary Fig. D and E for details on the transmission configuration. More details on the infrastructure cost calculations can be found in Supplementary Note 3.

In this study, we calculate the LCOE using both single and multiple site configurations. In the single site configuration, we calculate the LCOE associated with each individual grid cell and assume a dedicated transmission line to shore at Morehead City. In this layout, the total transmission distance equals the direct distance between Morehead City and the grid cell, and for the generation units installed in a single site, the total collection line consists of the spur lines for each separate 4 MW unit, which is an average 1 km given the spacing distance between turbines. In the multisite configuration, grid cells are selected using portfolio optimization and electricity output from each site is aggregated. In this layout, we optimize the collection point location using a Newton-Raphson iterative method such that the total cabling cost is minimized.

The mooring design includes mooring cables, anchors, and buoyancy tanks, which are used to provide undersea support. Therefore, the total mooring costs are affected by both the number of units installed and the sea floor depth (h) at each installed site. We followed Neary et al. [10] to calculate the total mooring cost, but modified the RM4 mooring design. In the RM4 design, the two-point mooring system consists of tension and thrust lines that are secured to the seafloor. However, the mooring lines are attached to only one point on the turbine unit, which does not prevent the unit from rotating about its vertical axis. Therefore, we include two additional tension lines and two additional thrust lines to balance the turbine from lateral current forces [58]. As a result, our cost coefficient for mooring material is three times as expensive as the estimate by Neary et al. [10].

The costs associated with deployment include the cable shore landing, mooring and foundation system, cable installation, and device installation. Again, estimates drawn from Neary et al. [10] are used. We linearly scaled these cost estimates for project sizes ranging from 4 MW to 400 MW to obtain deployment cost per unit of installed capacity.

Development costs mainly consist of siting and scoping, project design, engineering and management costs, and environmental compliance costs, such as permitting costs, National Environmental Policy Act (NEPA) compliance, and administrative costs. Logarithmic regression is applied to fit the development cost estimates as a function of capacity from Neary et al. [10].

O&M costs are associated with energy production and transmission on an ongoing basis. Annual fixed O&M costs are drawn from Neary et al. [10]. It includes O&M for marine operations, shore-based operations, replacement parts, and consumables. As with deployment and development, a linear scaling is applied to O&M costs.

3. Results

3.1. Gulf Stream resource assessment

As described in Section 2.1, we estimated annual capacity factors associated with marine turbines for all grid points within the study domain (77° W to 74° W, 33° N to 36° N). Fig. 2a–f shows the annual capacity factors and illustrate the significant spatiotemporal variability associated with hypothetical annual electricity production. The sites with the highest capacity factors from 2009 to 2011 are located in the southwestern quadrant whereas from 2012 to 2014 the highest capacity factors are found in the northeastern quadrant. Furthermore, the highest capacity factor in 2014 is over 80%, but the same site has a capacity factor of only 50% in 2011.

The average site-specific capacity factor over the six-year span (2009–2014) is depicted in Fig. 2g. Note that the site with the highest average six-year capacity factor is over 160 km away from Morehead City, the assumed grid tie-in point, and 230 km away from Cape Hatteras. The strongest currents with a capacity factor greater than 40% are concentrated between the isobaths of 100 m and 3000 m, since the stream flows over the upper continental slope before it traverses the Atlantic towards Northern Europe.

3.2. Correlation of current velocity and distance between sites

The significant inter-annual variability in capacity factor at a given location presents a serious economic challenge to potential investors who may experience years with little or no electricity production. One possible solution is to aggregate electricity generation from multiple sites.

To explore the possibility of turbine site diversification, we calculate the correlation in monthly electricity production from 2009 to 2014 between all grid cell pairs in the study domain. Since land is included in the study domain, the number of site pairs as a function of distance is not uniform (Supplementary Fig. A). Fig. 3 bins the correlation estimates by the nearest kilometer distance between grid cell pairs. The upper and lower edges indicate the maximum and minimum correlation, respectively, at the same integer distance; all other samples at the same distance fall within the shaded region.

The average coefficients in Fig. 3 indicate that as the distance between two sites increases, the average coefficient of correlation approaches zero. In addition, the lowest coefficients of correlation occur at distances between 50 and 150 km, which corresponds to the approximate width of the Gulf Stream within the studied domain. If two sites are situated such that one site is in the Gulf Stream current and the other is not, their monthly energy outputs will be more negatively correlated. Overall, the decreasing correlation as a function of distance implies that diversification of turbine sites over a wide geographic area could reduce the total variation in electricity production.

3.3. Portfolio optimization of generation sites

Based on the US Department of Energy's (DOE) reference model 4 (RM4) marine turbine design detailed in Neary et al. [10], each turbine unit has an installed capacity of 4 MW, and a single 2 km × 2 km grid cell can contain up to 16 MW of installed turbine capacity (See Supplementary Fig. B for more details.). To explore the optimal site locations associated with a larger installation, we conduct a portfolio optimization that requires a small but manageable 80 MW of total installed capacity across no more than 5 different locations.

As described in Section 2.2, the portfolio optimization model distributes installed capacity across different sites in order to

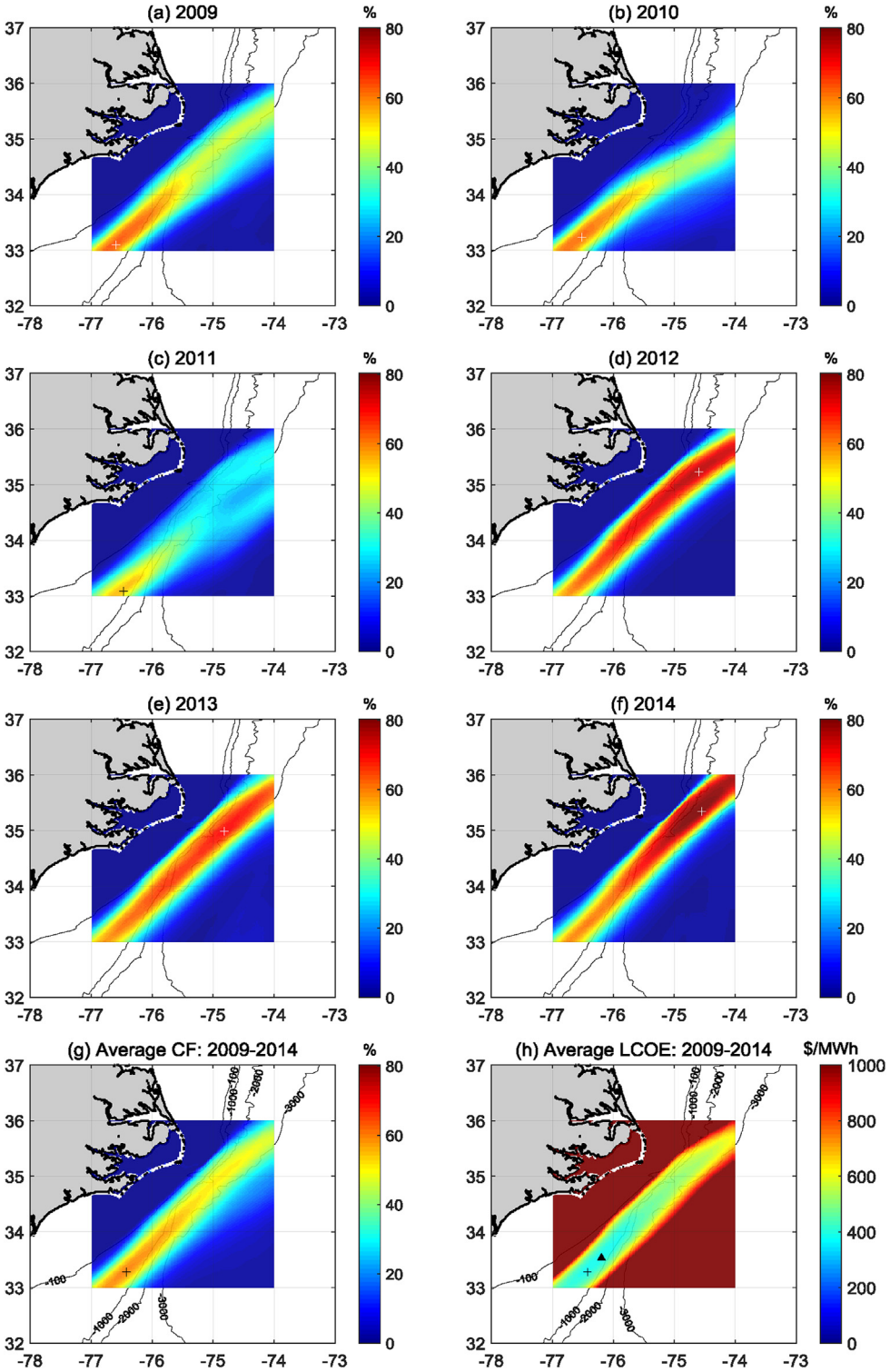

Fig. 2. Estimated capacity factor (a–g) and levelized cost of electricity (LCOE) (h) across the study domain. Crosses mark the locations with the highest annual capacity factors. Comparison of annual estimates indicates significant meanders and speed variations in the Gulf Stream. The triangle in (h) indicates the lowest LCOE. The 100 m, 1000 m, 2000 m and 3000 m bottom-depth contours (isobaths) are indicated by the black lines running southwest-to-northeast. The continental shelf is that portion of the ocean from the coastline to 100 m, and the continental slope extends seaward from the 100 m isobath.

minimize the variance in total monthly electricity output at an exogenously specified capacity factor target. In order to make the formulation computationally tractable, the portfolio optimization is performed in two stages. Fig. 4 presents the tradeoff between capacity factor and variance. The Stage 1 results represent the efficient frontier when there is no integer constraint on the number of installed generating units. The Stage 2 results represent the modified efficient frontier when the integer constraint on the number of generating units is placed on the candidate sites chosen in Stage 1.

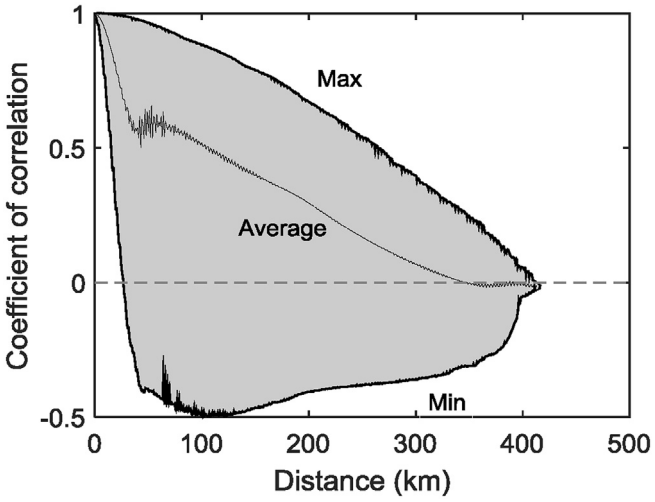

Fig. 3. Correlation in monthly electricity production versus distance for each pair of grid cells in the study domain. The correlation estimates are binned by distance to the nearest kilometer. The minimum, average, and maximum correlation coefficient at each distance are shown as lines; all other site pairs fall within the gray region.

For comparison, the dots represent the minimum variance at a given capacity factor target that can be obtained when only one grid cell is selected. The cross at the top of Fig. 4 marks the maximum 6-year average capacity factor among all the sites in the domain. The results illustrate that it is possible to significantly reduce the variance in energy output at a given capacity factor by creating a portfolio of geographically dispersed sites rather than relying on a single site. For example, among all individual sites with capacity factor equal to 40%, the minimum variance is approximately 60,000 $(\text{MWh/month})^2$, while the best portfolio can reduce the total variance approximately 20 times to 3000 $(\text{MWh/month})^2$.

The variance reductions through portfolio optimization, which are represented by the horizontal distances between the efficient frontier and the solid dots on Fig. 4, decrease as the required target capacity factor increases. When the target capacity factor is equal to the maximum capacity factor across all sites, there is only one grid cell left in the portfolio; the inclusion of any other grid cells fails to meet the target capacity factor. Thus, as the target capacity factor is increased, the potential reduction in covariance through site diversification is reduced. As expected, the gap between the Stage 1 and 2 frontiers in Fig. 4 implies that the addition of integer constraints slightly worsens the optimization results, since the portfolio variance increases. Furthermore, the addition of integer constraints in Stage 2 affect the achievable capacity factor, hence the misalignment between the Stage 1 and 2 capacity factor targets.

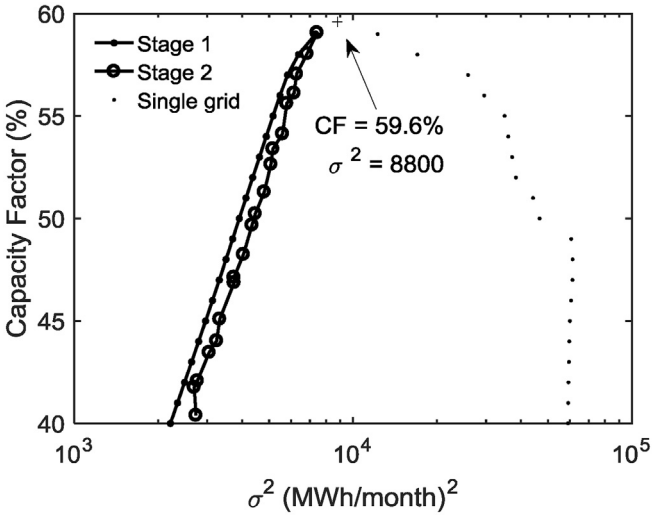

Fig. 4. Results from the portfolio optimization. Stage 1 results represent the optimal portfolio without an integer constraint on the number of turbine units, while Stage 2 results use the candidate sites selected from Stage 1 and include the integer constraint. The scattered dots to the right indicate the minimum variance among individual grid cells with the same capacity factor targets rounded to the nearest percent.

Fig. 5 shows the optimal site locations from portfolios with different target capacity factors. The selected sites range from the 100 m and 2500 m isobaths due to the bathymetry constraint based on limits to anchoring depth. The number of selected sites in each Stage 1 portfolio is less than 20, even though there are over 4000 candidate sites. In addition, most of the selected sites are clustered around the site with the highest six-year average capacity factor, represented by the cross. When the target capacity factor is low, the selected sites tend to spread out over a larger geographic area to take advantage of weaker correlations in output.

3.4. Levelized cost study

It is possible to formulate the portfolio optimization problem with a constraint on LCOE rather than capacity factor. However, such a formulation would lead to a more complex non-linear model due to the interaction between the capacity allocated to a specific site and the energy production from the turbines within the site, which in turn depends on the allocated capacity. Thus, while the portfolio study indicates the tradeoff between variability and total output, it does not take cost into account.

Fig. 2h presents the LCOE from individual sites and indicates that at the center of the Gulf Stream, the lowest LCOE is slightly above 400 $/MWh. Sites with the lowest LCOEs are located near the center of the Gulf Stream, which is consistent with Fig. 2g, since a higher site-specific capacity factor implies a lower LCOE. Interestingly, the site with the highest six-year average capacity factor is not the same as that with the lowest six-year average LCOE, as illustrated in Fig. 2h. The site with the lowest LCOE, indicated by a triangle, is closer to Morehead City, the assumed grid tie-in point, than the site with the highest six-year average capacity factor, as marked with a cross. The distance between the two sites is approximately 35 km. This represents the tradeoff between energy quality and transmission cost: it is more cost-effective to select a site with marginally lower resource quality but a shorter transmission distance.

The results depicted in Fig. 2 provide a useful visualization of the resource quality and LCOE over a continuous domain. To study the LCOE as a function of the cumulative amount of electricity generation from the Gulf Stream, supply curves for the years 2009–2014 are shown in Fig. 6. These curves represent the marginal cost to produce the next increment of electricity. As more electricity is generated, the cost to extract it becomes more expensive as locations with declining resource quality must be utilized. For simplicity, we assume that the addition of each new site requires dedicated transmission lines to Morehead City. In addition, we account for array losses by applying a scaling factor that reduces the output at each site by approximately 53%.[1] While a more accurate accounting of array losses would require modeling that accounts for the incremental array losses as new capacity is deployed, Fig. 6 nonetheless illustrates how inter-annual variability in the Gulf Stream resource affects LCOE. The LCOE at a given production level

[1] This estimate is drawn from Yang et al. [7] by comparing scenarios with zero drag coefficient (i.e., no array losses) and a uniform drag coefficient.

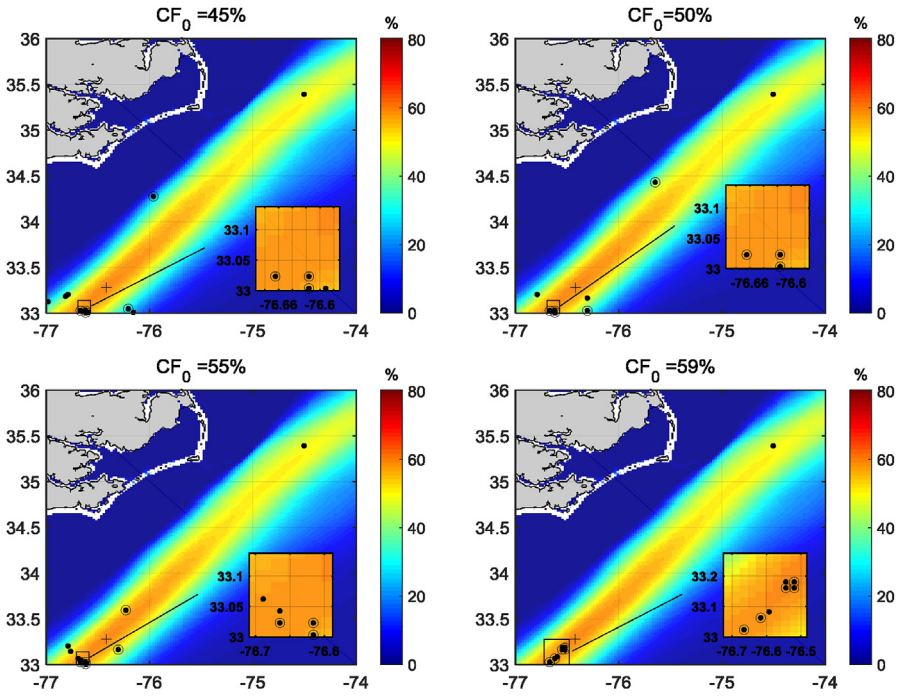

Fig. 5. Selected sites within the optimal portfolios at different minimum capacity factor targets. The filled circles on each figure indicate the location of installed capacity in Stage 1 solutions, while the open circles indicate installed capacity in Stage 2 solutions. For reference, the cross indicates the location of the site with the maximum six-year average capacity factor. The background color shading represents the six-year average capacity factors (CF) from 2009 to 2014, and the inset provides an expanded view of the selected sites near 33° N and 77° W.

can vary by more than 300 $/MWh from one year to the next. These results suggest that inter-annual variability in Gulf Stream intensity can have a significant impact on year-to-year costs and revenue.

While we did not directly constrain the LCOE in the portfolio optimization, Fig. 7a shows the LCOE calculated *ex post* as a function of the target capacity factor. Since we include project economies of scale based on Neary et al. [10], the portfolio-based LCOE with installed capacity of 80 MW is lower than that of a 16 MW single site; the entire LCOE profile in the former case is below 400 $/MWh. As expected, the LCOE is inversely correlated with capacity factor since higher capacity factors represent higher annual electricity production.

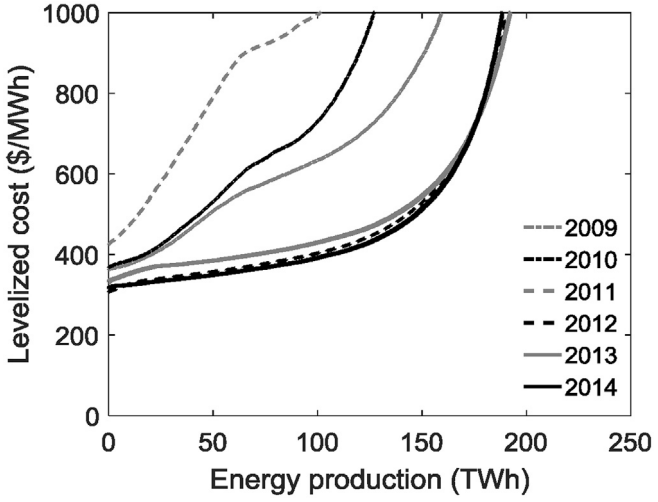

Fig. 6. Annual supply curves from 2009 to 2014. Significant inter-annual variability in LCOE at a given production level can be observed.

However, the LCOE is not monotonically decreasing with increasing capacity factor: the LCOE increases when the capacity factor increases from 46% to 47%, from 49% to 50% and from 52% to 53%. These variations are due to transmission cost, and to a lesser extent, mooring cost. Among all cost components, the power take-off and transmission infrastructure are the two principal cost drivers. Each time the target capacity factor increases, the model returns a new portfolio that includes a different set of sites with the same total installed capacity. Given the fixed installed capacity, the device structural components cost, power take-off cost, development cost and deployment cost remain the same, but the infrastructure cost will be affected by the transmission distance (see Supplementary Note 3). In addition, changing the site selection also affects the assumed depths, which in turn affect mooring cost. In some cases, the incremental increase in infrastructure and mooring cost outweighs the incremental increase in electricity production, and the LCOE increases with the capacity factor. Thus, while an increasing capacity factor target increases the energy yield, it does not guarantee a lower LCOE.

Fig. 7b compares the cost breakdown of the turbine arrays in both the single site and optimal portfolios by showing the percentage shares of each component contributing to the total annualized cost. The sample set associated with the single site case covers the whole sub-domain, while the optimal portfolio case only contains 20 optimal portfolios, representing the 20 different capacity factor targets (from 0.40 to 0.59). The wider spread in the single site layout indicates a broader range of transmission distances and mooring depths associated with the larger domain.

By contrast, the smaller ranges in Fig. 7b associated with the optimal portfolios reflect the much smaller sample size as well as the clustering of selected sites: most sites are grouped around the location with the highest average capacity factor, therefore the transmission distances are similar. The results indicate that power take-off components and transmission infrastructure are the two

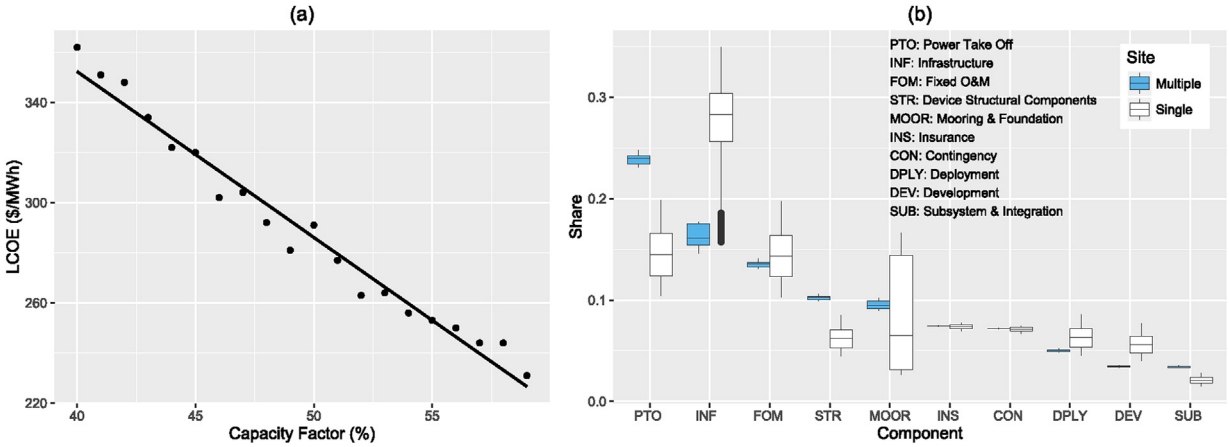

Fig. 7. LCOE analysis for the portfolios from the MVP model. (a) LCOE calculated *ex post* as a function of the capacity factor target in the portfolio optimization. (b) Box plot showing the share of LCOE attributable to different cost components in both the single site and portfolio cases, ordered from highest to lowest share in the portfolio case. The edges of each box represent the 25th and 75th percentiles, and the whiskers extend to the maximum and minimum values.

leading cost drivers. In addition, when the installed capacity increases from 16 MW in the single site to 80 MW in the portfolio, the percentage shares of infrastructure, deployment and development decrease due to the inclusion of project economies of scale for these components, which in turn lead to the increase of the percentage shares of device structural components and power take-off.

In the portfolio analysis, the estimated LCOE drops from 350 $/MWh to 230 $/MWh when the capacity factor increases from 40% to 59%. For comparison, Jenne et al. [36] estimate an LCOE of approximately 200 $/MWh for an 80 MW installation in the Florida Straits. The reason for the higher LCOE in the North Carolina case is twofold: capacity factors in the Florida Current are consistently around 70%, which is higher than even the best site in this study; and the transmission distances in North Carolina are significantly greater than in the Florida Straits. The average transmission distance from the collection point to Morehead City is around 160–180 km, compared with 30 km in the Florida Straits.

4. Discussion

The resource quality associated with Gulf Stream current energy off the North Carolina coast is highly variable. Fig. 2 shows that model-computed capacity factors exhibit significant spatiotemporal variability due to path meanders and speed variations in the Gulf Stream. Around 35° North latitude, the average location of the shoreward edge of the Gulf Stream moves from the 3000 m isobath in 2010 to between the 2000 and 3000 m isobaths in 2012, while the Gulf Stream position around 33° North remains fixed. This observation is consistent with previous studies [25,27,59], where the Gulf Stream's path is found to have similar inter-annual variations.

The optimized portfolio of generation sites, which aggregates electricity production from geographically diversified turbine units, can significantly reduce the variability in electricity generation and improve the economic prospects of the technology. Similar to wind farms, site diversification can reduce the need for back-up reserves. Fig. 5 indicates that as the target capacity factor increases, the selected sites cluster around the southwestern quadrant of the study domain where the site with the highest six-year average capacity factor is located. Another advantage of deploying turbine arrays in this region is that the lateral amplitude of the Gulf Stream meander is near a minimum within the domain [19,23–25,27,59–61]. For that portion of the Gulf Stream upstream of Cape Hatteras, the standard deviation of the surface front position increases northeastward from the “Charleston bump” and then decreases on towards Cape Hatteras due to the steepening of the continental slope approaching Cape Hatteras [19,23,24,27,62]. In addition, the envelope of the Gulf Stream meandering downstream of Cape Hatteras broadens to 200–300 km or more [25,60,61], greater than its own width of about 100 km, compared to the maximum lateral movement of around 40 km [19] from Charleston to Cape Hatteras. In summary, both the oceanographic study and the portfolio optimization indicate that the region containing the Gulf Stream currents approximately 200 km southwest of Cape Hatteras is the most cost-effective location to deploy turbines along the North Carolina coastline.

Several caveats should be noted. First, there are significant uncertainties associated with cost given the lack of commercial experience with this technology. Second, while the 6-year MABSAB ocean model hindcast dataset enables a critical examination of inter-annual variability in Gulf Stream energy resources, a longer record would help to better characterize the economic effects of meanders. Third, in this study, the LCOE associated with the optimal portfolios are calculated *ex post*. While Fig. 7a indicates that capacity factor is a reasonable proxy for LCOE, changes in the transmission and mooring costs can increase the LCOE at higher capacity factor targets.

A revised optimization model that makes LCOE rather than capacity factor the driving constraint would be preferable, but would result in a more complex non-linear model. The class of mixed-integer nonlinear optimization problems is one of the hardest to solve in the optimization literature [63], particularly when it is a constrained non-convex optimization model. According to Mansini et al. [63], there are no algorithms for the exact solution of non-convex nonlinear programming problems in which the feasible region is a mixed-integer set. This raises concerns about reaching a local instead of a global optimal [64] and requires exhaustive computational time or the use of a metaheuristic technique [65] to find an approximate solution when solving the model.

Gulf Stream energy off the North Carolina coast will not be a viable option without significant cost reductions: our model shows that the optimized portfolios have LCOEs ranging from 230 to 350 $/MWh. By comparison, Jenne et al. [36] estimated an LCOE of 200 $/MWh for ocean current energy in the Florida Straits, a tier-one site located 30 km east of Fort Lauderdale. Both estimates are still far higher than baseload sources such as coal, steam and natural gas combined cycle, which have LCOEs ranging from 70 to 100 $/MWh [66]. It is also not competitive with commercially mature

renewables such as solar photovoltaics and wind, which can be as low as 70 $/MWh [66]. Nonetheless, a range of technologies must be brought to bear on the global effort to mitigate climate change, and it is worth exploring technologies in the earliest stages of development, such as ocean current energy, which may become cost-effective in select locations with further innovation and reductions in manufacturing and deployment costs.

The ocean current turbine design drawn from DOE's RM4 utilizes off-the-shelf components, and there is reason to expect significant cost reductions with commercially optimized designs. Understanding the role of variable resource quality in determining levelized costs is critical to making ocean current energy part of a low-GHG generation future. While this analysis focuses on Gulf Stream resources off the North Carolina coast, the analysis provides a framework to examine the plausibility of extracting energy from other ocean currents characterized by temporal and geographical variability. The portfolio analysis can simply be repeated with resource data from other western boundary currents.

Acknowledgements

The authors acknowledge the support of the North Carolina Ocean Energy Program and the Department of Civil, Construction & Environmental Engineering at NC State University. The authors also wish to express their gratitude to Yanlin Gong from the Department of Marine, Earth, and Atmospheric Sciences at NC State University for performing the MABSAB ocean circulation hindcast, Mohammed Gabr and Md Ahsan Uz Zaman from the Department of Civil, Construction & Environmental Engineering at NC State University for their assistance with the anchoring system design, and Leonard White from the Department of Electrical and Computer Engineering at NC State University for his constructive advice on the transmission infrastructure.

Appendix A. Supplementary data

Supplementary data related to this article can be found at http://dx.doi.org/10.1016/j.energy.2017.06.048.

References

[1] Burman K, Walker A. Ocean energy technology overview. 2009.
[2] Ramon GZ, Feinberg BJ, Hoek EMV. Membrane-based production of salinity-gradient power. Energy Environ Sci 2011;4:4423–34. http://dx.doi.org/10.1039/C1EE01913A.
[3] Bedard R, Previsic M, Hagerman G, Polagye B, Musial W, Klure J, et al. North American ocean energy status—March 2007. In: 7th Eur. Wave tidal energy conf. (EWTEC), Porto, Port. Sept.; 2007. p. 11–3.
[4] U.S. Department of the Interior. Ocean current energy potential on the U.S. Outer continental shelf. 2006.
[5] Duerr AES, Dhanak MR. An assessment of the hydrokinetic energy resource of the Florida current. IEEE J Ocean Eng 2012;37:281–93.
[6] Lissaman PBS. The coriolis Program. Oceanus 1979;22:23–8.
[7] Yang X, Haas KA, Fritz HM. Evaluating the potential for energy extraction from turbines in the gulf stream system. Renew Energy 2014;72:12–21. http://dx.doi.org/10.1016/j.renene.2014.06.039.
[8] Jacobson PT, Hagerman G, Scott G. Mapping and assessment of the United States ocean wave energy resource. 2011.
[9] Haas KA, Fritz HM, French SP, Smith BT, Neary V. Assessment of energy production potential from tidal streams in the United States. 2011.
[10] Neary VS, Lawson M, Previsic M, Copping A, Hallett KC, Labonte A, et al. Methodology for design and economic analysis of marine energy conversion (MEC) technologies. 2014.
[11] Bane JM, He R, Muglia M, Lowcher CF, Gong Y, Haines SM. Marine hydrokinetic energy from western boundary currents. Ann Rev Mar Sci 2017;9. http://dx.doi.org/10.1146/annurev-marine-010816-060423.
[12] Yang X, Haas KA, Fritz HM, French SP, Shi X, Neary VS, et al. National geodatabase of ocean current power resource in USA. Renew Sustain Energy Rev 2015;44:496–507. http://dx.doi.org/10.1016/j.rser.2015.01.007.
[13] Chen F. Kuroshio power plant development plan. Renew Sustain Energy Rev 2010;14:2655–68. http://dx.doi.org/10.1016/j.rser.2010.07.070.
[14] Tsao C-C, Feng A-H, Hsieh C, Fan K-H. Marine current power with cross-stream active mooring: Part I. Renew Energy 2017;109:144–54. http://dx.doi.org/10.1016/j.renene.2017.02.065.
[15] Marais E, Chowdhury S, Chowdhury SP. Theoretical resource assessment of marine current energy in the Agulhas Current along South Africa's East coast. 2011 IEEE Power Energy Soc Gen Meet 2011:1–8. http://dx.doi.org/10.1109/PES.2011.6039502.
[16] Meyer I, Niekerk JL Van. Towards a practical resource assessment of the extractable energy in the Agulhas ocean current. Int J Mar Energy 2016;16:116–32. http://dx.doi.org/10.1016/j.ijome.2016.05.010.
[17] Williams A, Nthontho M, Chowdhury S, Chowdhury SP. Modelling South african Agulhas marine current profile data for electricity generation. In: Power syst. Technol. (POWERCON), 2012 IEEE int. Conf.; 2012. p. 1–7. http://dx.doi.org/10.1109/PowerCon.2012.6401419.
[18] VanZwieten Jr JH, Duerr AES, Alsenas GM, Hanson HP. Global ocean current energy assessment: an initial look. In: Proc. 1rd Mar. Energy technol. Symp. (METS13), Washington, DC, USA; 2013. p. 10–1.
[19] Bane JM, Brooks DA. Gulf stream meanders along the continental margin from the Florida Straits to Cape Hatteras. Geophys Res Lett 1979;6:280–2. http://dx.doi.org/10.1029/GL006i004p00280.
[20] Usui N, Wakamatsu T, Tanaka Y, Hirose N, Toyoda T, Nishikawa S, et al. Four-dimensional variational ocean reanalysis: a 30-year high-resolution dataset in the western North Pacific (FORA-WNP30). J Oceanogr 2017;73:205–33. http://dx.doi.org/10.1007/s10872-016-0398-5.
[21] Hsin Y-C, Qiu B, Chiang T-L, Wu C-R. Seasonal to interannual variations in the intensity and central position of the surface Kuroshio east of Taiwan. J Geophys Res Ocean 2013;118:4305–16. http://dx.doi.org/10.1002/jgrc.20323.
[22] Elipot S, Beal LM. Characteristics, energetics, and origins of Agulhas current meanders and their limited influence on ring shedding. J Phys Oceanogr 2015;45:2294–314. http://dx.doi.org/10.1175/JPO-D-14-0254.1.
[23] Zeng X, He R. Gulf Stream variability and a triggering mechanism of its large meander in the South Atlantic Bight. J Geophys Res Ocean 2016;121:8021–38. http://dx.doi.org/10.1002/2016JC012077.
[24] Gula J, Molemaker MJ, McWilliams JC. Gulf stream dynamics along the southeastern U.S. Seaboard. J Phys Oceanogr 2015;45:690–715. http://dx.doi.org/10.1175/JPO-D-14-0154.1.
[25] Andres M. On the recent destabilization of the Gulf Stream path downstream of Cape Hatteras. Geophys Res Lett 2016;43:9836–42. http://dx.doi.org/10.1002/2016GL069966.
[26] Bryden HL, Beal LM, Duncan LM. Structure and transport of the Agulhas current and its temporal variability. J Oceanogr 2005;61:479–92. http://dx.doi.org/10.1007/s10872-005-0057-8.
[27] Olson DB, Brown OB, Emmerson SR. Gulf Stream frontal statistics from Florida Straits to Cape Hatteras derived from satellite and historical data. J Geophys Res Ocean 1983;88:4569–77. http://dx.doi.org/10.1029/JC088iC08p04569.
[28] Rourke FO, Boyle F, Reynolds A. Marine current energy devices: current status and possible future applications in Ireland. Renew Sustain Energy Rev 2010;14:1026–36. http://dx.doi.org/10.1016/j.rser.2009.11.012.
[29] Myers LE, Bahaj AS. An experimental investigation simulating flow effects in first generation marine current energy converter arrays. Renew Energy 2012;37:28–36. http://dx.doi.org/10.1016/j.renene.2011.03.043.
[30] Bahaj AS, Myers LE. Fundamentals applicable to the utilisation of marine current turbines for energy production. Renew Energy 2003;28:2205–11. http://dx.doi.org/10.1016/S0960-1481(03)00103-4.
[31] Bahaj AS, Molland AF, Chaplin JR, Batten WMJ. Power and thrust measurements of marine current turbines under various hydrodynamic flow conditions in a cavitation tunnel and a towing tank. Renew Energy 2007;32:407–26. http://dx.doi.org/10.1016/j.renene.2006.01.012.
[32] Bahaj AS, Batten WMJ, McCann G. Experimental verifications of numerical predictions for the hydrodynamic performance of horizontal axis marine current turbines. Renew Energy 2007;32:2479–90. http://dx.doi.org/10.1016/j.renene.2007.10.001.
[33] Batten WMJ, Bahaj AS, Molland AF, Chaplin JR. The prediction of the hydrodynamic performance of marine current turbines. Renew Energy 2008;33:1085–96. http://dx.doi.org/10.1016/j.renene.2007.05.043.
[34] Batten WMJ, Bahaj AS, Molland AF, Chaplin JR. Hydrodynamics of marine current turbines. Renew Energy 2006;31:249–56. http://dx.doi.org/10.1016/j.renene.2005.08.020.
[35] Fraenkel PL. Marine current turbines: pioneering the development of marine kinetic energy converters. Proc Inst Mech Eng Part A J Power Energy 2007;221:159–69.
[36] Jenne DS, Yu YH, Neary V. Levelized cost of energy analysis of marine and hydrokinetic reference models. In: Proc. 3rd Mar. Energy technol. Symp. (METS15), Washington, DC, USA; 2015.
[37] Kabir A, Lemongo-Tchamba I, Fernandez A. An assessment of available ocean current hydrokinetic energy near the North Carolina shore. Renew Energy 2015;80:301–7. http://dx.doi.org/10.1016/j.renene.2015.02.011.
[38] Gong Y, He R, Gawarkiewicz GG, Savidge DK. Numerical investigation of coastal circulation dynamics near Cape Hatteras, North Carolina, in January 2005. Ocean Dyn 2015;65:1–15.
[39] Mellor GL, Yamada T. Development of a turbulence closure model for geophysical fluid problems. Rev Geophys 1982;20:851–75. http://dx.doi.org/10.1029/RG020i004p00851.
[40] Chassignet EP, Hurlburt HE, Smedstad OM, Halliwell GR, Hogan PJ, Wallcraft AJ, et al. The HYCOM (HYbrid Coordinate Ocean Model) data

assimilative system. J Mar Syst 2007;65:60–83. http://dx.doi.org/10.1016/j.jmarsys.2005.09.016.
[41] Luettich Jr RA, Westerink JJ, Scheffner NW. ADCIRC: an advanced three-dimensional circulation model for shelves, coasts, and Estuaries. Report 1. Theory and Methodology of ADCIRC-2DDI and ADCIRC-3DL. 1992.
[42] Chen K, He R. Mean circulation in the coastal ocean off northeastern North America from a regional-scale ocean model. Ocean Sci Discuss 2014;11:2755–90.
[43] Xue Z, Zambon J, Yao Z, Liu Y, He R. An integrated ocean circulation, wave, atmosphere, and marine ecosystem prediction system for the South Atlantic Bight and Gulf of Mexico. J Oper Oceanogr 2015;8:80–91.
[44] Markowitz HM, Todd GP. Mean-variance analysis in portfolio choice and capital markets. John Wiley & Sons; 2000.
[45] Drake B, Hubacek K. What to expect from a greater geographic dispersion of wind farms?—A risk portfolio approach. Energy Policy 2007;35:3999–4008. http://dx.doi.org/10.1016/j.enpol.2007.01.026.
[46] Roques F, Hiroux C, Saguan M. Optimal wind power deployment in Europe—a portfolio approach. Energy Policy 2010;38:3245–56. http://dx.doi.org/10.1016/j.enpol.2009.07.048.
[47] Reichenberg L, Johnsson F, Odenberger M. Dampening variations in wind power generation—the effect of optimizing geographic location of generating sites. Wind Energy 2014;17:1631–43. http://dx.doi.org/10.1002/we.1657.
[48] Santos-Alamillos FJ, Thomaidis NS, Usaola-García J, Ruiz-Arias JA, Pozo-Vázquez D. Exploring the mean-variance portfolio optimization approach for planning wind repowering actions in Spain. Renew Energy 2017;106:335–42. http://dx.doi.org/10.1016/j.renene.2017.01.041.
[49] Novacheck J, Johnson JX. Diversifying wind power in real power systems. Renew Energy 2017;106:177–85. http://dx.doi.org/10.1016/j.renene.2016.12.100.
[50] Degeilh Y, Singh C. A quantitative approach to wind farm diversification and reliability. Int J Electr Power Energy Syst 2011;33:303–14. http://dx.doi.org/10.1016/j.ijepes.2010.08.027.
[51] Thomaidis NS, Santos-Alamillos FJ, Pozo-Vázquez D, Usaola-García J. Optimal management of wind and solar energy resources. Comput Oper Res 2016;66:284–91. http://dx.doi.org/10.1016/j.cor.2015.02.016.
[52] Westner G, Madlener R. Development of cogeneration in Germany: a mean-variance portfolio analysis of individual technology's prospects in view of the new regulatory framework. Energy 2011;36:5301–13. http://dx.doi.org/10.1016/j.energy.2011.06.038.
[53] Tjelta TI, others. Suction piles: their position and application today. In: Elev. Int. Offshore polar eng. Conf.; 2001.
[54] Power Verdant. Final kinetic hydro power pilot license application, Roosevelt Island tidal energy project. FERC No. 12611. 2010.
[55] Li B, DeCarolis JF. A techno-economic assessment of offshore wind coupled to offshore compressed air energy storage. Appl Energy 2015;155:315–22.
[56] Green J, Schellstede H. Electrical collection and transmission systems for offshore wind power. In: Offshore technol. Conf. Houston, Texas, April 30 – May 3, Houston, Texas; 2007.
[57] The University of North Carolina at Chapel Hill. Coastal wind: energy for North Carolina's future. 2009. Chapel Hill, North Carolina.
[58] Ahsanuzzaman M, Gabr M, DeCarolis JF. Quantifying the effects of meanders on Gulf stream electricity costs. Raleigh, North Carolina. 2016.
[59] Miller JL. Fluctuations of gulf stream frontal position between Cape Hatteras and the Straits of Florida. J Geophys Res Ocean 1994;99:5057–64. http://dx.doi.org/10.1029/93JC03484.
[60] Tracey KL, Watts DR. On gulf stream meander characteristics near Cape Hatteras. J Geophys Res Ocean 1986;91:7587–602. http://dx.doi.org/10.1029/JC091iC06p07587.
[61] Watts DR, Johns WE. Gulf Stream meanders: observations on propagation and growth. J Geophys Res 1982;87:9467–76.
[62] Brooks DA, Bane JM. Gulf stream deflection by a bottom feature off Charleston, South Carolina. Sci (80-) 1978;201:1225–6.
[63] Mansini R, Ogryczak W, Speranza MG. Twenty years of linear programming based portfolio optimization. Eur J Oper Res 2014;234:518–35. http://dx.doi.org/10.1016/j.ejor.2013.08.035.
[64] Murty KG, Kabadi SN. Some NP-complete problems in quadratic and nonlinear programming. Math Program 1987;39:117–29. http://dx.doi.org/10.1007/BF02592948.
[65] Crama Y, Schyns M. Simulated annealing for complex portfolio selection problems. Eur J Oper Res 2003;150:546–71. http://dx.doi.org/10.1016/S0377-2217(02)00784-1.
[66] US Energy Information Administration. Annual energy outlook. 2015. p. 2015.